ELSEVIER

Coordination Chemistry Reviews
211 (2001) 117–144

COORDINATION CHEMISTRY REVIEWS

www.elsevier.com/locate/ccr

Structure, NMR and other physical and photophysical properties of ruthenium(II) complexes containing the 3,3′-dicarboxyl-2,2′-bipyridine ligand

B.-Z. Shan, Q. Zhao, N. Goswami, D.M. Eichhorn *[1], D.P. Rillema *[2]

Department of Chemistry, Wichita State University, Wichita, KS 67260-0051, USA

Received 14 September 1999; accepted 10 January 2000

Dedicated to Arthur Adamson on the occasion of his 80th birthday

Contents

[1] *Corresponding author.
[2] *Corresponding author. Tel.: +1-316-9783120; fax: +1-316-9783431; e-mail: rillema@wsuhub.uc.twsu.edu

PII: S0010-8545(00)00286-1

Abstract

A series of compounds of the type $[(bpy)_2Ru(3,3'\text{-XX-}2,2'\text{-bpy})]^{2+}$ or $[(dmb)_2Ru(3,3'\text{-XX-}2,2'\text{-bpy})]^{2+}$, where X is CH_2OH, COOH, $COOCH_3$, $COOC_2H_5$, and $COOCH_2C_6H_5$ and bpy and dmb are 2,2′-bipyridine and 4,4′-dimethyl-2,2′-bipyridine, respectively, have been synthesized. $[Ru(bpy)_2((COOCH_3)_2bpy)](PF_6)_2\cdot 2CH_3CN$ crystallized in the monoclinic space group $P2_1/c$ with $a = 15.347$ (3), $b = 22.767$ (4), $c = 12.971$ (3) Å, and $Z = 4$. ^{1}H-NMR spectra were assigned. The proton on the carbon atom neighboring the nitrogen coordination site shifts upfield upon coordination to ruthenium(II). Electronic absorptions occur over the visible region from 550 to 400 nm, which are attributed to metal-to-ligand charge transfer and in the UV region from 250 to 350 nm, which are associated with intraligand processes. The absorbance in the visible region of the spectrum displays two components, $Ru(d\pi) \rightarrow \pi^*(bpy)$ and $Ru(d\pi) \rightarrow \pi^*((COOR)_2bpy)$ for $R = CH_3$, C_2H_5 and $CH_2C_6H_5$, in the other cases the $Ru(d\pi) \rightarrow \pi^*$ transitions to the three bipyridine ligands overlap. Reduction potentials attributed to the Ru(III/II) couple range from 1.22 V for the CH_2OH derivative to 1.40 V versus SSCE for the $COOC_2H_5$ derivative. Reductions attributed to the first reduction of the coordinated (3,3′-XX-2,2′-bpy) ligand occur over the range -0.88 to -1.36 V versus SSCE. Emission maxima at room temperature in acetonitrile range from 614 nm for the CH_2OH derivative to 711 nm for the ester derivatives; their emission lifetimes at room temperature in acetonitrile vary from 940 to 258 ns, respectively.

Keywords: NMR; Ruthenium(II) complexes; 3,3′-Dicarboxyl-2,2′-bipyridine ligand

1. Introduction

Considerable attention has focused on the preparation and properties of ruthenium(II) heterocyclic ligand complexes due to their stability and photophysical properties. Such complexes ranging from simple monometallic to larger arrays have been reviewed by a number of contributors in the area [1–3]. Complexes of this

type are of high interest from both a fundamental point of view where the dynamics of excited state electron and energy transfer are under investigation and from a practical point of view where photochemical devices related to light-to-energy conversion have been proposed or devised [4–10].

We have pioneered the use of multidentate heterocyclic ligands for the preparation of mixed-metal and multimetallic complexes [11–14] and have studied applications of these complexes as catalysts in solar photoelectrochemical cells [15,16]. Our most recent reports in the area have been related to monometallic and bimetallic complexes based on 4,5-diazafluorenone [17–20]. Nucleophiles in solutions containing ruthenium(II) coordinated to 4,5-diazafluorenone attacked the carbonyl carbon atom, opened the five-membered ring and resulted in new complexes containing bipyridine ligands substituted in the 3 position. This allowed us to prepare and investigate the properties of $[Ru(bpy)_2(3\text{-}COOHbpy)]^{2+}$ and then extend our studies to ruthenium(II) complexes with substituents in the 3,3′ positions of one of the three bipyridine ligands for subsequent use as dyes in solar energy cells. The presence of these substituents in close proximity was expected to result in steric distortions as well as the normal Hammett σ donor–acceptor effects. Here we vary the substituents from the electron donating group, CH_2OH, to the electron withdrawing groups, COOR, where R = H, CH_3, C_2H_5 and CH_2Ph, and show that molecular distortions are another means for altering physical properties of ruthenium(II) complexes. The structures of the various ligands used are shown in Fig. 1.

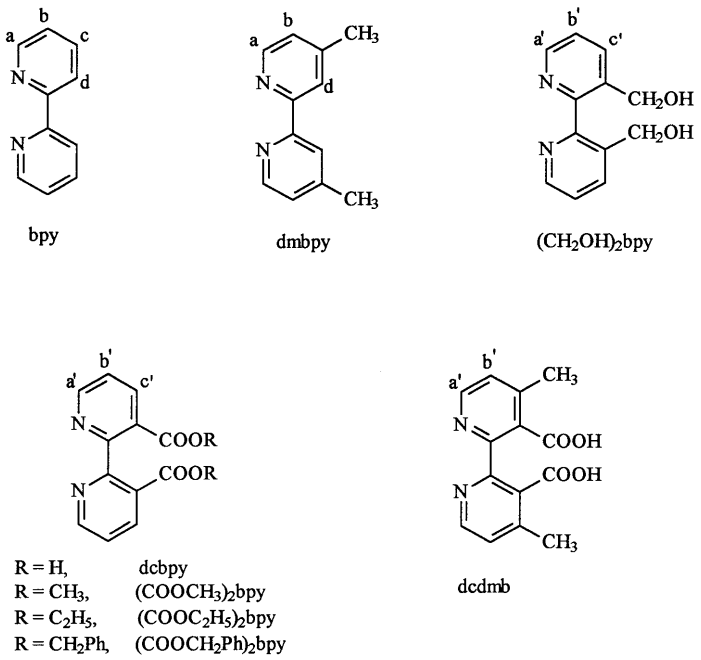

Fig. 1. Structures of various ligands, abbreviations, and labels for ^{1}H-NMR assignments.

2. Experimental

2.1. Materials

Ruthenium trichloride trihydrate was obtained on loan from Johnson–Mathey. Argon and nitrogen gases were purchased from Lightner Welding. Tetrabutylammonium hexafluorophosphate (TBAH) was purchased from Southwestern Analytical Chemicals and was stored in a desiccator. Silver trifluoromethanesulfonate (silver triflate or AgTFMS) was purchased from Aldrich and stored in a vacuum desiccator in the dark. Methanol, tetrahydrofuran, acetonitrile, methylene chloride, chloroform, and ethanol were purchased from Fisher.

Methanol and ethanol were dried by placing 5 g of clean, dry magnesium turnings and 0.5 g of iodine in a flask under argon gas, followed by 50–75 ml of commercially purchased absolute methanol or ethanol. The mixture was warmed until the iodine disappeared. Commercial absolute methanol or ethanol (900 ml) was then added and the solution was refluxed for 30 min. The methanol or ethanol was then distilled directly into the reaction vessel.

Tetrahydrofuran (THF) was refluxed under argon gas in the presence of sodium–potassium alloy and benzophenone until a blue color formed. The solvent remained in contact with the alloy until it was distilled for use.

Reagents used in the preparation of 3,3′-dicarboxy-2,2′-bipyridine, 3,3′-dicarboxy-4,4′-dimethyl-2,2′-bipyridine, 3,3′-dicarbomethoxy-2,2′-bipyridine, 3,3′-dicarboethoxy-2,2′-bipyridine, 3,3′-dicarbobenzoxy-2,2′-bipyridine and 3,3′-dimethylol-2,2′-bipyridine were purchased from G.F. Smith or Aldrich and were used without further purification.

cis-Dichlorobis(2,2′-bipyridine)ruthenium(II) and *cis*-dichlorobis(4,4′-dimethyl-2,2′-bipyridine)ruthenium(II)were prepared according to published procedures [21].

Elemental analyses were carried out by M-H-W Laboratories, Phoenix, AZ.

2.2. Preparation of 3,3′-dicarboxy-2,2′-bipyridine, dcbpy

A modification of the procedure of Smith and Richer was followed [22]. A sample of 1,10-phenanthroline (8.0 g, 0.04 mol) was added to a 2 l round bottomed flask containing 800 ml of distilled water and 3.2 g (0.08 mol) of NaOH. Potassium permanganate crystals (19.0 g, 0.12 mol) were then slowly added at room temperature (r.t.) using a powder dropping funnel while stirring the solution. After the addition, the solution was refluxed for at least 2 h. The resulting mixture was filtered while hot to remove the MnO_2. The filtrate was reduced to half of its original volume and it was acidified using acetic acid. Silver nitrate (13.6 g) was then dissolved in a minimum amount of distilled water and slowly added to concentrated filtrate with stirring. The resulting white precipitate was collected by filtration and was added to 500 ml boiling distilled water. The boiling mixture was saturated with hydrogen sulfide gas (hydrogen sulfide was obtained by the reaction of solid sodium sulfide and 6 M hydrochloric acid) [22]. Black silver sulfide precipitated from the solution. Hydrogen sulfide was bubbled through the solution

until the solution appeared to be clear and the black precipitate began to clump together. The mixture was filtered while hot and a slightly yellow colored solution was obtained. The solution was decolorized with carbon while the solution was boiling. A clear solution was obtained after filtration. The filtrate was reduced to 20 ml and a white solid precipitated from the solution. The precipitate was collected and dried in a vacuum oven. A 4.26 g (0.017 mol, 43.6%) yield of white product was obtained. The compound decomposed within the range 250–252°C. ^{1}H-NMR (DMSO, ppm): δ 12.95 (s, 2H, COOH); 8.66 (d, 2H); 8.26 (d, 2H); 7.52 (dd, 2H). Anal. Calc. for $C_{12}H_8N_2O_4$: C, 59.02; H, 3.30; N, 11.47. Found: C, 59.38; H, 3.12; N, 11.41%.

2.3. Preparation of 3,3′-dicarbomethoxy-2,2′-bipyridine, [(COOCH$_3$)$_2$bpy]

A 3.65 g (0.015 mol) sample of 3,3′-dicarboxy-2,2′-bipyridine was dissolved in 110 ml of freshly distilled methanol containing 3.29 ml (0.030 mol) of *N*-methylmorpholine. The solution was placed in an ice-bath for at least 10 min and 2.31 ml (0.030 mol) of methylchloroformate was added dropwise over a period of 20 min. The whole procedure was performed under an argon atmosphere. The solution was then stirred at r.t. for at least 30 min and the solvent was removed using a rotary evaporator. The solid residue was dissolved in 110 ml chloroform. This solution was washed three times with 25 ml portions of saturated sodium bicarbonate. The chloroform layer was concentrated by rotary evaporation. A white crystalline product precipitated from the solution. The solid was removed by filtration and washed with a small amount of cold, absolute ethanol. The crystalline product was dried in a vacuum oven overnight. A 3.02 g (0.0111 mol, 73.90%) yield of product was obtained. M.p.: 153–155°C (lit. m.p. 152°C) [23]. IR (KBr, cm^{-1}): C–H, 2950; Ar–H, 3100. ^{1}H-NMR ($CDCl_3$, ppm): δ 8.75 (d, 2H); 8.35 (d, 2H); 7.43 (dd, 2H); 3.65 (s, 6H).

2.4. Preparation of 3,3′-dicarboethoxy-2,2′-bipyridine, [(COOCH$_2$CH$_3$)$_2$bpy]

A similar procedure to that used to prepare 3,3′-dicarbomethoxy-2,2′-bipyridine was used for synthesizing 3,3′-dicarboethoxy-2,2′-bipyridine. The solvent was freshly distilled ethanol instead of distilled methanol. M.p.: 84–86°C. IR (KBr, cm^{-1}): C–H, 2985; Ar–H, 3100 cm^{-1}. ^{1}H-NMR ($CDCl_3$, ppm): δ 8.75 (d, 2H); 8.35 (d, 2H); 7.40 (dd, 2H); 4.10 (q, 4H); 1.05 (t, 6H). Anal. Calc. for $C_{16}H_{16}N_2O_4$: C, 63.99; H, 5.37: N, 9.33. Found: C, 63.55; H, 5.31; N, 9.18%.

2.5. Preparation of 3,3′-dicarbobenzoxy-2,2′-bipyridine, [(COOCH$_2$Ph)$_2$bpy]

A mixture of 2.44 g (0.01 mol) 3,3′-dicarboxy-2,2′-bipyridine, 4.54 g (0.022 mol) *N*,*N*-dicyclohexylcarbodiimide, 2.38 g (0.022 mol) benzyl alcohol and 0.29 g (0.002 mol) 4-pyrrolidinopyridine in dichloromethane (40 ml) was magnetically stirred 16 h at r.t. under argon gas until esterification was complete. The *N*,*N*-dicyclohexylurea which formed was removed by filtration and the filtrate was washed with

distilled water (3×40 ml), 5% acetic acid solution (3×40 ml), and again with distilled water (3×40 ml). The methylene chloride layer was separated from the water layer and dried with $MgSO_4$. The solvent was then evaporated slowly in a fume hood. A 3.47 g (0.0081 mol) (yield, 82%) sample of white crystals was collected and dried in the vacuum oven. M.p.: 84–86°C. IR (KBr, cm^{-1}): C–H, 2985; Ar–H, 3100. ^{1}H-NMR (CD_3CN, ppm): δ 8.57 (d, 2H); 8.18 (d, 2H); 7.38 (dd, 2H); 7.29 (m, 6H); 7.11 (m, 4H); 5.05 (s, 4H). Anal. Calc. for $C_{26}H_{20}N_2O_4$: C, 73.57; H, 4.75; N, 6.60. Found: C, 73.66; H, 5.00; N, 6.71%.

2.6. Preparation of 3,3′-dimethylol-2,2′-bipyridine, [(CH$_2$OH)$_2$bpy]

A 1.31 g (0.0048 mol) of 3,3′-dicarbomethoxy-2,2′-bipyridine was dissolved in 130 ml of freshly distilled THF under argon gas. The solution was placed in an ice-bath for at least 10 min. A solution of Red Al (sodium bis[2-methoxyethoxy]-aluminum(hydride)) containing 0.021 mol of reagent was prepared with 20 ml of freshly distilled THF. This solution was added dropwise into the reaction mixture in a period of 30 min. After 1 h at 0°C, the excess Red Al reagent was decomposed by slow addition of a saturated aqueous NH_4Cl solution. $CHCl_3$ (100 ml) was then added and the resulting liquid was decanted. The residue was washed with 3×100 ml of $CHCl_3$. The organic layers were combined, dried, and rotary evaporated to dryness yielding a tan colored solid which was recrystallized in ethyl acetate resulting in 0.64 g (0.0030 mol, 62% yield) of product. M.p.: 144–146°C (lit. m.p. 144–145°C) [24]. IR (KBr, cm^{-1}): C–H, 2950; Ar–H, 3100. ^{1}H-NMR (DMSO, ppm): δ 8.52 (d, 2H); 8.05 (d, 2H); 7.49 (dd, 2H); 5.25 (t, 2H); 4.35 (d, 4H).

2.7. Preparation of 3,3′-dicarboxy-4,4′-dimethyl-2,2′-bipyridine, dcdmb

A 9.0 g (0.04 mol) sample of 4,7-dimethyl-1,10-phenanthroline was added to a 2 l round bottom flask containing 1200 ml of distilled water and 4.8 g (0.12 mol) of NaOH. Potassium permanganate (19.0 g, 0.12 mol) was then slowly added at r.t. After the addition, the solution was stirred a r.t. for 20 h, then refluxed for 2 h. The resulting mixture was filtered. The filtrate was reduced to about one quarter of its volume and acidified using acetic acid. After filtering, the filtrate was treated with a solution of silver nitrate (9.0 g) and H_2S as above, and then decolorized with carbon. The solid was collected by reducing the filtrate volume to near dryness, and then recrystallized twice using a 1:1 water–ethanol mixture. A white product was obtained (2.6 g, 0.0095 mol, yield 23.9%). ^{1}H-NMR (D_2O, ppm): δ 8.56 (d, 2H); 7.76 (d, 2H); 2.61 (s, 6H). Anal. Calc. for $C_{14}H_{12}N_2O_4 \cdot H_2O$: C, 57.93; H, 4.86; N, 9.32. Found: C, 58.26; H, 4.87; N, 9.32%.

2.8. Preparation of [(bpy)$_2$Ru(dcbpy-H)](PF$_6$)

cis-Dichlorobis(2,2′-bipyridine)ruthenium(II) (0.2600 g, 0.5 mmol) and 3,3′-dicarboxy-2,2′-bipyridine (0.1221 g, 0.5 mmol) were refluxed in 50 ml ethanol for 6 h.

While still hot, the solution was filtered. The filtrate was concentrated to dryness using a rotary evaporator. A small amount of distilled water was added to dissolve the solid and the resulting solution was loaded onto a cation exchange chromatography column (Sephadex SP-25, Pharmacia, 40–120 mesh) and the complex was eluted with an aqueous solution of sodium chloride. The first fraction obtained with pure distilled water contained an impurity and was discarded. The fraction obtained with 0.2 M sodium chloride contained the desired complex. The complex was then precipitated by adding saturated aqueous NH_4PF_6 solution. It gave one spot on a silica gel TLC plate using 5:4:1 acetonitrile–water–saturated KNO_3(aq) as the developing reagent. M.p.: 227–229°C. IR (KBr, cm^{-1}): PF_6^-, 837. Anal. Calc. for $RuC_{32}H_{23}N_6O_4PF_6 \cdot H_2O$: C, 46.89; H, 3.05; N, 10.25. Found: C, 46.95, H, 2.88; N, 10.17%.

2.9. Preparation of $[(bpy)_2Ru((COOCH_3)_2bpy)](PF_6)_2$

cis-Dichlorobis(2,2′-bipyridine)ruthenium(II) (0.2600 g, 0.5 mmol) and 3,3′-dicarbomethoxy-2,2′-bipyridine (0.1361 g, 0.5 mmol) were refluxed in 50 ml ethanol for 6 h. While still hot, the solution was filtered. The filtrate was concentrated to dryness using a rotary evaporator. A small amount of distilled water was added to dissolve the solid and a saturated aqueous NH_4PF_6 solution was added to the above solution. The reddish-brown colored precipitate was collected on a fine frit, washed with distilled water and then with ethyl ether. The solid was dried in a vacuum oven overnight. The solid was dissolved in acetonitrile and a small amount of ethyl ether was slowly added. The mixture was placed in the refrigerator for several days. A small crystalline cluster grew from the solution which gave one spot on a silica gel TLC plate using 5:4:1 acetonitrile–water–saturated KNO_3(aq) as the developing reagent. M.p.: 286–287°C. IR (KBr, cm^{-1}): PF_6^-, 837. ^{1}H-NMR in the aliphatic region (CD_3CN, ppm): δ 3.80 (s, 6H). Anal. Calc. for $RuC_{34}H_{28}N_6O_4P_2F_{12}$: C, 41.86; H, 2.89; N, 8.61. Found: C, 41.01; H, 3.03; N, 7.65%.

2.10. Preparation of $[(bpy)_2Ru((COOCH_2CH_3)_2bpy)](PF_6)_2$

cis-Dichloro-bis(2,2′-bipyridine)ruthenium(II) (0.2600 g, 0.5 mmol) and 3,3′-dicarboethoxy-2,2′-bipyridine (0.1501 g, 0.5 mmol) were refluxed in 50 ml ethanol for 6 h. While still hot, the solution was filtered. The filtrate was concentrated to dryness using a rotary evaporator. A small amount of distilled water was added to dissolve the solid and a saturated aqueous NH_4PF_6 solution was added to the above solution. The reddish-brown colored precipitate was collected on a fine frit, washed with distilled water and then with ethyl ether. The solid was dried in a vacuum oven overnight. The solid was dissolved in acetonitrile and a small amount of ethyl ether was slowly added. The mixture was placed in a refrigerator for several days. A small crystalline cluster grew from the solution. It gave one spot on a silica gel TLC plate using 5:4:1 acetonitrile–water–saturated KNO_3(aq) as the developing reagent. M.p.: 254–255°C. IR (KBr): PF_6^-, 841 cm^{-1}. ^{1}H-NMR in the aliphatic

region (CD_3CN, ppm): δ 4.31 ppm (q, 4H); 1.25 ppm (t, 6H). Anal. Calc. for $RuC_{36}H_{32}N_6O_4P_2F_{16}$: C, 43.08; H, 3.21; N, 8.37. Found: C, 43.22; H, 3.12; N, 8.38%.

2.11. Preparation of $[(bpy)_2Ru((COOCH_2Ph)_2bpy)](PF_6)_2$

cis-Dichlorobis(2,2′-bipyridine)ruthenium(II) (0.2600 g, 0.5 mmol) and 3,3′-dicarbobenzoxy-2,2′-bipyridine (0.212 g, 0.5 mmol) were refluxed in 50 ml ethanol for 6 h. While still hot, the solution was filtered. The filtrate was concentrated to dryness using a rotary evaporator. A small amount of distilled water was added to dissolve the solid and a saturated aqueous NH_4PF_6 solution was added to the above solution. The reddish-brown colored precipitate was collected on a fine frit, washed with distilled water and then with ethyl ether. The procedures outlined in the previous preparation were used to purify the complex. M.p.: 205–207°C. IR (KBr, cm^{-1}): PF_6^-, 841. ^{1}H-NMR in the aliphatic region (CD_3CN, ppm): δ 5.27 ppm (s, 2H). Anal. Calc. for $RuC_{46}H_{36}N_6O_4P_2F_{12}\cdot H_2O$: C, 48.21; H, 3.32; N, 7.33. Found: C, 48.41; H, 4.17; N, 7.01%.

2.12. Preparation of $[(bpy)_2Ru((CH_2OH)_2bpy)](PF_6)_2$

cis-Dichlorobis(2,2′-bipyridine)ruthenium(II) (0.2600 g, 0.5 mmol) and 3,3′-dimethylol-2,2′-bipyridine (0.1081g, 0.5 mmol) were refluxed in 50 ml ethanol for 6 h. While still hot, the solution was filtered. The filtrate was concentrated to dryness using a rotary evaporator. A small amount of distilled water was added to dissolve the solid and a saturated aqueous NH_4PF_6 solution was added. An orange colored precipitate was collected. The procedures outlined for preparing $[(bpy)_2Ru((COOCH_2CH_3)_2bpy)](PF_6)_2$ were used to purify the complex. M.p.: 213–215°C. IR (KBr, cm^{-1}): PF_6^-, 841. ^{1}H-NMR in the aliphatic region (CD_3CN, ppm): δ 3.8 (t, 2H); 4.6 (d, 4H). Anal. Calc. for $RuC_{32}H_{28}N_6O_2P_2F_{12}$: C, 41.79; H, 3.07; N, 9.14. Found: C, 42.00; H, 3.32; N, 9.30%.

2.13. Preparation of $[Ru(dmb)_2(dcdmb)](PF_6)_2$

A 0.20 g sample of dcdmb (0.74 mmol) and 0.41 g of $Ru(dmb)_2Cl_2$ (0.74 mmol) were refluxed in 80 ml ethanol for 10 h. The solution was filtered. The filtrate was evaporated to dryness using a rotary evaporator. A small amount of distilled water was added to dissolve the solid and the resulting solution was loaded onto a cation exchange chromatography column (Sephadex SP-25, 40–120 mesh) and the complex was eluted with an aqueous solution of sodium chloride. The fraction obtained with 0.2 M NaCl contained the desired complex. The complex was precipitated by adding HPF_6. The solid was then recrystallized from acetone. The yield was 0.2 g (26.5%). ^{1}H-NMR in the aliphatic region (CD_3CN, ppm): δ 2.45 (s, 6H); 2.49 (6H); 2.22 (6H). Anal. Calc. for $RuC_{38}H_{36}N_6O_4P_2F_{12}$: C, 44.24%; H, 3.52; N, 8.15. Found: C, 44.66; H, 2.55; N, 8.23%.

2.14. Preparation of $[Ru(dmb)_2(dcbpy\text{-}H)](PF_6)$

A 0.29 g sample of $Ru(dmb)_2Cl_2$ (0.5 mmol) and 0.12 g dcbpy (0.5 mmol) were added to a 100 ml flask containing 60 ml ethanol. The resulting solution was refluxed for 6 h and then filtered. The filtrate was evaporated to dryness. The solid was dissolved in a small amount of water and loaded onto a cation exchange column (Sephadex SP-25, 40–120 mesh) and the complex was eluted with an aqueous solution of sodium chloride. The fraction obtained with 0.2 M NaCl contained the desired complex. The complex was precipitated by the dropwise addition of saturated NH_4PF_6. A pure complex (0.25 g) was obtained by recrystallizing the product in acetone (yield = 49.8%). ^{1}H-NMR in the aliphatic region (CD_3CN, ppm): δ 2.45 (12 H). Anal. Calc. for $RuC_{36}H_{31}N_6O_4PF_6$: C, 50.34; H, 3.64; N, 9.79. Found: C, 50.40; H, 3.12; N, 9.80%.

2.15. Physical measurements

UV–vis spectra were obtained using a Hewlett–Packard model 8452A diode array spectrophotometer. IR spectra were obtained using a Perkin–Elmer model 1600 FT-IR spectrophotometer. Proton NMR spectra were obtained with Varian XL-300 and Varian Inova 400 FT-NMR spectrometers. Cyclic voltammograms were obtained using an EG&G PAR model 263A potentiostat/galvanostat. The measurements were made in a typical H-cell using a platinum disk working electrode, a platinum wire counter electrode and a silver/silver chloride reference electrode in acetonitrile. The supporting electrolyte was 0.1 M tetrabutylammonium hexafluorophosphate (TBAH).

Emission spectra were obtained using a Spex Fluorolog 212 spectrofluorometer using either 4:1 ethanol–methanol, methylene chloride or acetonitrile as solvent. All emission spectra were corrected for instrument response. Excited-state lifetimes were determined by exciting the sample at 450 nm using a frequency tripled Continuum Surlite ND:YAG laser run at $\sim$20 mJ/10 ns pulse. Oscilloscope control and data curve fitting were accomplished with a program developed in-house. Emission quantum yields were determined using $[Ru(bpy)_3]^{2+}$ as a standard which has a known emission quantum yield of 0.062 at 25°C [25] in acetonitrile. All emission samples were prepared in HPLC or better grade solvents, filtered through 0.45 PTFE filters, then freeze–pump–thaw degassed a minimum of three times prior to measurement. Errors were $\pm$1 in the last digit, unless otherwise indicated.

Sample preparation for photophysical measurements involved dissolving a small amount of sample ($\sim$2 mg) in the appropriate solvent and the absorbance of the solution was measured. The concentration of the solution was altered in order to achieve an absorbance of about 0.10 at 450 nm. Such a concentration provides enough material for data acquisition but excludes any self-quenching processes from occurring. A 3–4 ml aliquot of the solution was then placed in a 10 mm diameter Suprasil (Heraeus) non-fluorescent quartz tube equipped with a tip-off manifold. The sample was then freeze–pump–thaw degassed for at least three cycles (to approximately 75 millitorr) removing any gases from the sample. The

manifold was then closed and the sample was allowed to equilibrate to r.t. Solvent evaporation was assumed to be negligible, therefore concentrations were assumed to remain constant throughout this procedure. Measurements at 77 K were performed by direct immersion of the sample tube in a suprasil Dewer flask filled with liquid nitrogen.

Emission quantum yields were then calculated using Eq. (1) [26].

$$\phi = (A_o/A_s)(I_s/I_o)\phi_{std} \quad (1)$$

In Eq. (1), I_o is the integral of the standard emission envelope, I_s is the integral of the sample emission envelope, A_o is the absorbance of the standard, A_s is the absorbance of the sample, ϕ is the emission quantum yield of the sample and ϕ_{std} is the emission quantum yield of the standard.

2.16. X-ray structure determination

A red needle of $[Ru(bpy)_2((COOCH_3)_2bpy)](PF_6)_2 \cdot 2CH_3CN$ with dimensions $0.60 \times 0.25 \times 0.15$ mm was affixed with Paratone-N oil (Exxon) to the end of a glass fiber mounted on a goniometer head and transferred to the cold stream of the diffractometer. X-ray data were collected at -110°C on an Enraf–Nonius CAD-4 diffractometer using graphite monochromated Mo–K_α radiation ($\lambda = 0.71069$ Å) and controlled by a Silicon Graphics O2 computer. The unit cell dimensions were determined from the setting angles of 24 reflections with $20 < \theta < 22°$. The crystal system was determined to be monoclinic and the space group was uniquely determined to be $P2_1/c$. Data were collected for one quadrant with $+h$, $+k$, $\pm l$, and $2 \leq 2\theta \leq 45°$ by the ω-scan mode. Relevant data collection parameters are given in Table 1. The structure was solved by direct methods [27] and refined by full-matrix least-squares techniques using the TEXSAN crystallographic package [28]. The data were corrected for Lorentz and polarization effects, as well as by an empirical absorption correction using the program DIFABS [29]. All non-hydrogen atoms were refined anisotropically. Hydrogen atoms were included at idealized positions but were not refined. Neutral atom scattering factors and anomalous dispersion factors were used as supplied in the TEXSAN package [30,31].

3. Results

3.1. Preparation of compounds

An outline for the synthesis of the ligands is shown in Scheme 1. The procedure for the 3,3′-dicarboxy-2,2′-bipyridyl synthesis was taken from Smith and Richter [22]. The yield was approximately the same as that reported in the literature. The procedure for the synthesis of 3,3′-dicarbomethoxy-2,2′-bipyridine, 3,3′-dicarboethoxy-2,2′-bipyridine, and 3,3′-dimethylol-2,2′-bipyridine reported by Rebek [24]

Table 1
Crystallographic data for $[Ru(bpy)_2((3,3'\text{-}COOCH_3)_2bpy)](PF_6)_2 \cdot 2CH_3CN$

Formula	$C_{38}H_{34}N_8O_4P_2F_{12}Ru$
Formula weight	1057.74
Space group	$P2_1/c$
a (Å)	15.347(3)
b (Å)	22.767(4)
c (Å)	12.971(3)
β (°)	112.69(2)
V (Å^3)	4181(2)
Z	4
Number of data ($I>2\sigma(I)$)	4214
Number of parameters	586
D_{calc} (g cm^{-3})	1.680
T (°C)	−110
Wavelength (Å)	0.71069
μ(Mo–K$_\alpha$) (cm^{-1})	5.57
R[a]	0.051
R_w[b]	0.057
S[c]	3.32
Max. and min. peak (e Å^{-3})	0.63 and −0.88
Trans. factors	0.8506–1.000

[a] $R = \Sigma \| |F_o| - |F_c| \| / \Sigma |F_o|$.
[b] $R_w = [\Sigma w(|F_o| - |F_c|)^2 / \Sigma w F_o^2]^{1/2}$, $w = [\sigma_c^2(F_o)]^{-1}$.
[c] $S = [\Sigma w(|F_o| - |F_c|)^2 / (N_o - N_v)]^{1/2}$.

was followed. The overall yield was approximately 10% lower than the yield reported.

The general procedure for the synthesis of the complexes follows: A 1:1 molar ratio mixture of the appropriate ruthenium dichloro precursor and the 3,3′-X,X-2,2′-bipyridine or dcdmb ligand in absolute ethanol was refluxed under argon about 6 h, during which time the violet solution became more red–orange indicating formation of the complex. After isolation, two different methods of purification were used. First, the carboxalate derivatives were purified by loading them onto a cation exchange chromatography column (Sephadex SP-25, Pharmacia, 40–120 mesh) and eluting the desired fraction with an aqueous NaCl solution. The remaining complexes were purified on a neutral alumina (50–70) column, eluting the desired fraction by gradually increasing the acetonitrile:toluene ratio. Purification of the diester derivatives on a neutral alumina column was a better purification method than the cation exchange method because the yield for the ester complex decreased when eluted through the aqueous NaCl solution, perhaps due to hydrolysis. The three ester complexes were further purified by recrystallization in a mixture of acetonitrile and diethyl ether. A dark reddish crystal cluster was collected in each case.

3.2. X-ray structure

An ORTEP [32] drawing of the $[Ru(bpy)_2(COOCH_3)_2bpy)]^{2+}$ cation is shown in Fig. 2. Final fractional atomic coordinates and equivalent isotropic thermal displacement parameters for the non-hydrogen atoms are given in Table 2, and selected bond distances and angles are given in Table 3. The $[Ru(bpy)_2(COOCH_3)_2$-

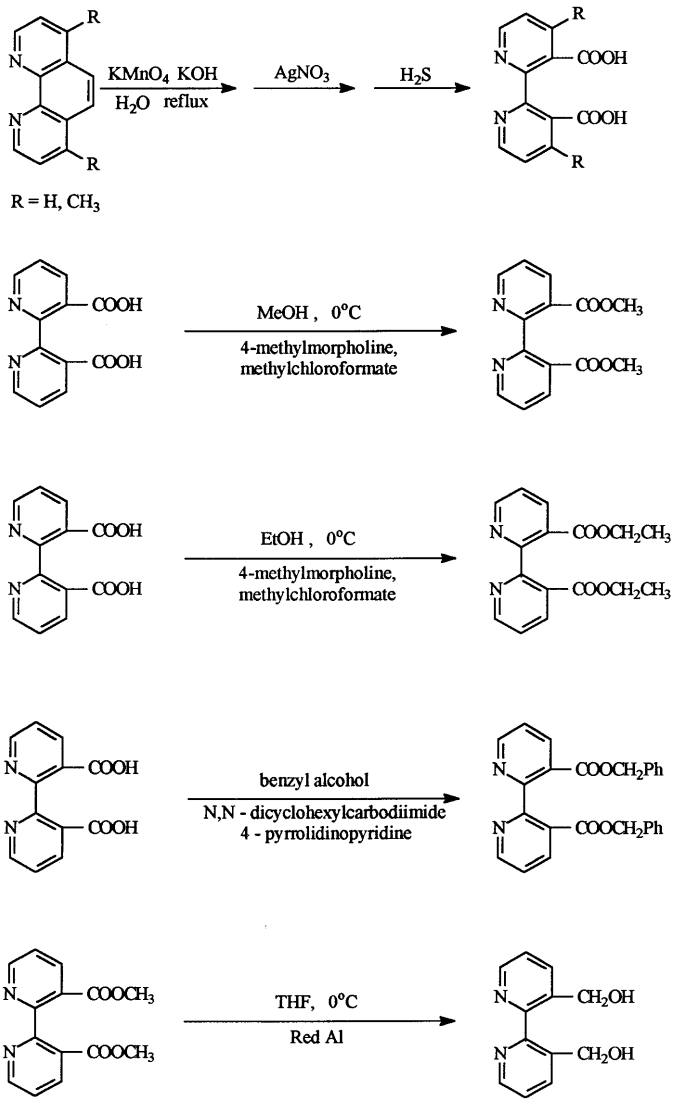

Scheme 1. Scheme for the synthesis of 3,3′-X,X-2,2′-bipyridine.

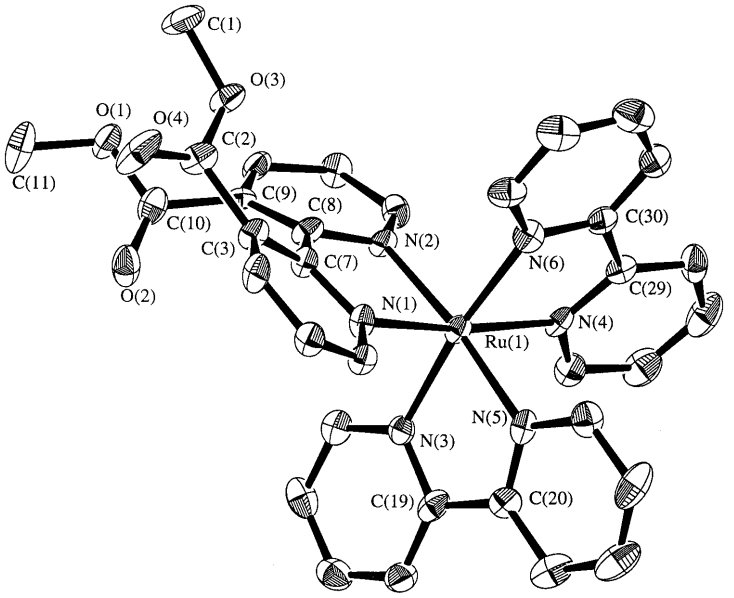

Fig. 2. ORTEP drawing of the $[Ru(bpy)_2((COOCH_3)_2bpy)]^{2+}$ cation. Ellipsoids are drawn at the 50% probability level and hydrogen atoms have been omitted for clarity.

bpy)]$^{2+}$ cation is found on a general position in the monoclinic space group $P2_1/c$. The asymmetric unit is completed by two hexafluorophosphate counterions and two molecules of acetonitrile.

The coordination geometry of the Ru atom is that of a distorted octahedron with a RuN_6 core. Four nitrogen atoms belong to two 2,2′-bipyridine ligands which lie in the *cis* configuration and the other two to the derivatized 2,2′-bipyridine ligand with methyl ester groups in the 3,3′ positions. The distortion from octahedral symmetry results from the small bite angles of the bipyridine ligands and the different bond distances to the various coordinating ligands. The N(1)–Ru–N(2) bite angle was 78.2 (2)°; the N(3)–Ru–N(5) bite angle was 78.4 (3)°; and the N(4)–Ru–N(6) bite angle was 78.5 (3)°. The distances of Ru–N varied from 2.052 (6) Å for Ru–N(4), 2.055 (6) Å for Ru–N(1), 2.059 (6) Å for Ru–N(2), 2.067 (6) Å for Ru–N(5), 2.080 (6) Å for Ru–N(6) to 2.084 (6) Å for Ru–N(3). The shortest distances on an average were to the derivatized 2,2′-bipyridine ligand with methyl ester groups in the 3,3′ positions. The bipyridine ligands are distorted with dihedral angles of 2.3° between the pyridine rings defined by N(4) and N(6), 6.6° between the pyridine rings defined by N(3) and N(5) and 28.1° between the pyridine rings defined by N(1) and N(2). The distances between the bridge-head carbon atoms of the bipyridine rings remained nearly constant ranging from 1.47 to 1.50 Å and the distances from the aromatic ring to the carbonyl carbon atoms were the same within experimental error, 1.49 (1) and 1.503 (9) Å.

Table 2
Positional parameters and B_{eq} for $[Ru(bpy)_2((3,3'\text{-}COOCH_3)_2bpy)](PF_6)_2 \cdot 2CH_3CN$

Atom	x	y	z	B_{eq}
Ru(1)	0.26053(5)	−0.12522(3)	0.73721(5)	1.57(1)
O(1)	0.1456(4)	−0.3987(2)	0.7384(4)	2.4(1)
O(2)	0.1410(4)	−0.3459(2)	0.5912(5)	2.9(2)
O(3)	0.3491(4)	−0.3557(2)	0.8170(4)	2.2(1)
O(4)	0.3618(5)	−0.3955(3)	0.6679(5)	4.7(2)
N(1)	0.2945(4)	−0.1926(3)	0.6541(5)	1.7(2)
N(2)	0.2212(4)	−0.1978(3)	0.8037(5)	1.5(2)
N(3)	0.1299(4)	−0.1165(3)	0.6052(5)	1.8(2)
N(4)	0.2404(5)	−0.0619(3)	0.8384(5)	1.5(2)
N(5)	0.2844(4)	−0.0545(3)	0.6517(5)	1.8(2)
N(6)	0.3922(4)	−0.1235(3)	0.8684(5)	2.0(2)
C(1)	0.3733(7)	−0.4118(4)	0.8760(7)	3.3(2)
C(2)	0.3485(6)	−0.3543(4)	0.7141(7)	2.2(2)
C(3)	0.3350(5)	−0.2940(3)	0.6647(6)	1.7(2)
C(4)	0.3821(6)	−0.2841(4)	0.5970(7)	2.3(2)
C(5)	0.3836(6)	−0.2288(4)	0.5526(6)	2.1(2)
C(6)	0.3404(5)	−0.1843(3)	0.5864(6)	1.7(2)
C(7)	0.2853(5)	−0.2479(3)	0.6887(6)	1.6(2)
C(8)	0.2243(5)	−0.2501(3)	0.7556(6)	1.7(2)
C(9)	0.1711(5)	−0.2977(3)	0.7640(6)	1.5(2)
C(10)	0.1520(6)	−0.3494(4)	0.6883(7)	2.2(2)
C(11)	0.1229(7)	−0.4499(4)	0.6666(8)	3.7(3)
C(12)	0.1258(6)	−0.2939(3)	0.8371(7)	2.0(2)
C(13)	0.1298(5)	−0.2426(4)	0.8960(6)	2.0(2)
C(14)	0.1761(5)	−0.1956(4)	0.8740(6)	1.9(2)
C(15)	0.0553(6)	−0.1518(4)	0.5833(7)	2.2(2)
C(16)	−0.0269(6)	−0.1435(4)	0.4922(7)	2.5(2)
C(17)	−0.0347(6)	−0.0971(4)	0.4208(7)	2.6(2)
C(18)	0.0405(6)	−0.0605(4)	0.4436(7)	2.4(2)
C(19)	0.1220(6)	−0.0704(3)	0.5347(7)	2.1(2)
C(20)	0.2078(6)	−0.0340(4)	0.5655(6)	2.0(2)
C(21)	0.2125(6)	0.0170(4)	0.5109(7)	2.7(2)
C(22)	0.2973(7)	0.0476(4)	0.5466(8)	3.4(3)
C(23)	0.3743(7)	0.0262(4)	0.6309(9)	3.5(3)
C(24)	0.3654(6)	−0.0244(4)	0.6835(7)	2.4(2)
C(25)	0.1593(6)	−0.0318(4)	0.8145(7)	2.2(2)
C(26)	0.1525(7)	0.0143(4)	0.8806(8)	3.0(2)
C(27)	0.2298(7)	0.0296(4)	0.9733(8)	3.3(3)
C(28)	0.3136(6)	−0.0014(4)	1.0007(7)	2.6(2)
C(29)	0.3171(6)	−0.0467(3)	0.9302(7)	1.9(2)
C(30)	0.4014(6)	−0.0828(4)	0.9467(7)	2.1(2)
C(31)	0.4860(6)	−0.0761(4)	1.0377(7)	2.6(2)
C(32)	0.5622(6)	−0.1119(4)	1.0497(7)	3.2(2)
C(33)	0.5501(6)	−0.1530(4)	0.9687(7)	3.0(2)
C(34)	0.4658(6)	−0.1581(4)	0.8804(7)	2.3(2)

Table 3
Selected bond lengths (Å) and angles (°) for $[Ru(bpy)_2((COOCH_3)_2bpy)](PF_6)_2 \cdot 2CH_3CN$

Bond lengths			
Ru(1)–N(1)	2.055(6)	C(29)–C(30)	1.48(1)
Ru(1)–N(2)	2.059(6)	C(19)–C(20)	1.47(1)
Ru(1)–N(3)	2.084(6)	C(2)–C(3)	1.50(1)
Ru(1)–N(4)	2.052(6)	C(7)–C(8)	1.503(9)
Ru(1)–N(5)	2.067(6)	C(9)–C(10)	1.49(1)
Ru(1)–N(6)	2.080(6)	O(3)–C(1)	1.461(9)
O(1)–C(10)	1.321(9)	O(3)–C(2)	1.332(9)
O(1)–C(11)	1.45(1)	O(4)–C(2)	1.172(9)
O(2)–C(10)	1.207(9)		
Bond angles			
N(1)–Ru(1)–N(2)	78.2(2)	N(5)–Ru(1)–N(6)	96.1(3)
N(1)–Ru(1)–N(3)	89.9(2)	N(4)–Ru(1)–N(6)	78.5(3)
N(1)–Ru(1)–N(4)	172.6(3)	N(4)–Ru(1)–N(5)	84.1(2)
N(1)–Ru(1)–N(5)	99.6(2)	N(3)–Ru(1)–N(6)	173.4(2)
N(1)–Ru(1)–N(6)	94.6(3)	N(3)–Ru(1)–N(5)	78.4(3)
N(2)–Ru(1)–N(3)	94.3(2)	N(3)–Ru(1)–N(4)	97.2(2)
N(2)–Ru(1)–N(4)	99.0(2)	N(2)–Ru(1)–N(6)	91.3(2)
N(2)–Ru(1)–N(5)	172.5(2)		

Table 4
Specific IR stretches for the complexes and ligands

Complexes/ligands	COOH (cm^{-1})	C=O (cm^{-1})	O–H (cm^{-1})
$[Ru(bpy)_2(dcbpy\text{-}H)](PF_6)$	2750–3600	1720	
$[Ru(dmb)_2(dcbpy\text{-}H)](PF_6)$	3421	1716	
dcbpy	2500–3400	1717	
$[Ru(dmb)_2(dcdmb)](PF_6)_2$	3425	1735	
dcdmb	3300–3500	1696	
$[(bpy)_2Ru((COOCH_3)_2bpy)](PF_6)_2$		1733	
$(COOCH_3)_2bpy$		1712	
$[(bpy)_2Ru((COOC_2H_5)_2bpy)](PF_6)_2$		1732	
$(COOC_2H_5)_2bpy$		1724	
$[(bpy)_2Ru((COOCH_2Ph)_2bpy)](PF_6)_2$		1731	
$(COOCH_2Ph)_2bpy$		1717	
$[(bpy)_2Ru((CH_2OH)_2bpy)](PF_6)_2$			3579
$(CH_2OH)_2bpy$			3251

3.3. IR spectra

The characteristic vibrations for the complexes and the free ligands are tabulated in Table 4. The FT-IR spectra of free ligands containing C=O groups displayed a strong absorption in the 1700 cm^{-1} region, which was absent for the 3,3′-$(CH_2OH)_2bpy$ derivative. The ligands with the COOH groups gave a broad absorption centered at 2912 cm^{-1}. Ligands containing the O–H group displayed

the characteristic O–H absorption between 3200 and 3500 cm^{-1}, which was absent for the ester derivatives. An absorption located in the 1500–1600 cm^{-1} region characteristic of bipyridine units was present in all the compounds. This absorption, located at 1574 cm^{-1} for 3,3′-$(COOH)_2$bpy, splits into two absorptions for the other free ligands with one peak located at approximately 1579 cm^{-1} and the second peak located near 1560 cm^{-1}.

The [Ru(bpy)$_2$(dcbpy-H)](PF_6) compound showed the characteristic COOH absorption in the region between 2750 and 3600 cm^{-1}. The absorption was shifted towards higher energy compared with the free ligand where the corresponding COOH stretch occurred between 2500 and 3400 cm^{-1}. The C=O stretches for the complex and the free ligand occurred at similar positions near 1600 cm^{-1}. The [Ru(bpy)$_2$((CH_2OH)$_2$bpy](PF_6)$_2$ complex showed an O–H stretch at 3579 cm^{-1} which is at higher energy compared with the O–H stretch of the free ligand located at 3251 cm^{-1}. The [Ru(bpy)$_2$(3,3′-(ester)$_2$bpy)](PF_6)$_2$ derivatives showed a C=O stretch at 1732 cm^{-1} for the three different ester complexes. The stretches were shifted towards higher energy compared with the C=O stretches of the free ligands, which occurred at 1712, 1724 and 1717 cm^{-1} for the methyl ester, ethyl ester and benzyl ester, respectively.

3.4. ^{1}H-NMR spectra

Data for proton assignments according to the symbols used in Fig. 1 are listed in Table 5. Assignments of ^{1}H signals in the aromatic region were determined by examining COSY spectra, as shown in Fig. 3, for [Ru(bpy)$_2$(dcbpy-H)](PF_6), by comparing coupling constants and by comparing spectra of complexes with ligands containing methyl substituents in the 4,4′ positions to spectra for complexes containing ligands with protons in those sites. These procedures were used to make unambiguous assignments for the acid derivatives and then these assignments were used by analogy for the ester derivatives. According to the data, the a and a′ proton resonances are most affected upon coordination. These shift upfield by over 0.5 ppm. The consequence of this results in the c, c′ and d proton resonances lying furthermost down field for these complexes since coordination of ruthenium does not affect their resonances as dramatically.

3.5. UV–vis spectra

A summary of the important UV–vis features are given in Table 6. Spectra are shown in Fig. 4 for four complexes. The extinction coefficients were obtained from Beer's law studies and were determined from at least four points. Absorptions were located across the UV–vis region commencing at approximately 550 nm. Three distinct peaks and two shoulders were observed. The peaks were located in the 420–450, 280–290 and 240 nm regions. Shoulders were found at about 500 and 320 nm. The assignments for the absorption bands were made on the basis of the well documented optical transitions in $[Ru(bpy)_3]^{2+}$ [33,34]. The very obvious shoulders around 500 nm for the three ester complexes were assigned as $d\pi \rightarrow \pi^*$(bpy-ester)

Table 5
^{1}H-NMR aromatic proton assignments in D_2O

Compound	H, a	H, b	H, c	H, d	H, a′	H, b′	H, c′
dcbpy					8.68 (d)	7.53 (dd)	8.27 (d)
dcdmb					8.56 (d)	7.76 (d)	
$[Ru(bpy)_2(dcbpy\text{-}H)]^+$	7.77 (d)	7.35 (dd)	8.05 (dd)	8.53 (d)	7.91 (d)	7.35 (dd)	8.22 (d)
	8.05 (d)	7.45 (dd)					
$[Ru(dmb)_2(dcbpy\text{-}H)]^+$	7.17 (d)	7.53 (d)		8.33 (s)	7.89 (d)	7.32 (dd)	8.16 (d)
	7.65 (d)						
$[Ru(dmb)_2(dcdmb)]^{2+}$	7.51 (d)	7.24 (d)		8.32 (s)	7.85 (d)	7.15 (d)	
	7.65 (d)	7.15 (d)					
$[Ru(bpy)_2((CH_2OH)_2bpy)]^{2+}$	7.76 (d)	7.33 (dd)	8.02 (dd)	8.51(d)	7.80 (d)	7.38 (dd)	8.04 (d)
$[Ru(bpy)_2((COOCH_3)_2bpy)]^{2+}$	7.42 (d)	7.40 (dd)	8.07 (dd)	8.49 (d)	7.89 (d)	7.45 (dd)	8.28 (d)
	7.65 (d)						
$[Ru(bpy)_2((COOCH_2CH_3)_2bpy)]^{2+}$	7.42 (d)	7.40 (dd)	8.08 (dd)	8.50 (d)	7.88 (d)	7.44 (dd)	8.29 (d)
	7.65 (d)						
$[Ru(bpy)_2((COOCH_2Ph)_2bpy)]^{2+}$	7.37 (d)	7.36 (dd)	8.05 (dd)	8.47 (d)	7.83 (d)	7.38 (dd)	8.22 (d)
	7.62 (d)						

transitions. The absorbances between 430–460 nm were assigned to metal-to-ligand charge transfer (MLCT) transitions ($d\pi \rightarrow \pi^*$(bpy)). The second transitions at higher energy between 280–290 nm were assigned to ligand centered charge transfer which were consistent with other reported LC ($\pi \rightarrow \pi^*$) transitions for these type of complexes [35,36]. The MLCT transitions between 450–500 nm follow the energy trend: $[Ru(bpy)_2((CH_2OH)_2bpy)]^{2+} > [Ru(bpy)_2(dcbpy\text{-}H)]^{+} > [Ru(bpy)_2((COOMe)_2bpy)]^{2+} \sim [Ru(bpy)_2((COOEt)_2bpy)]^{2+} \sim [Ru(bpy)_2((COO\text{-}CH_2Ph)_2bpy)]^{2+}$ [37].

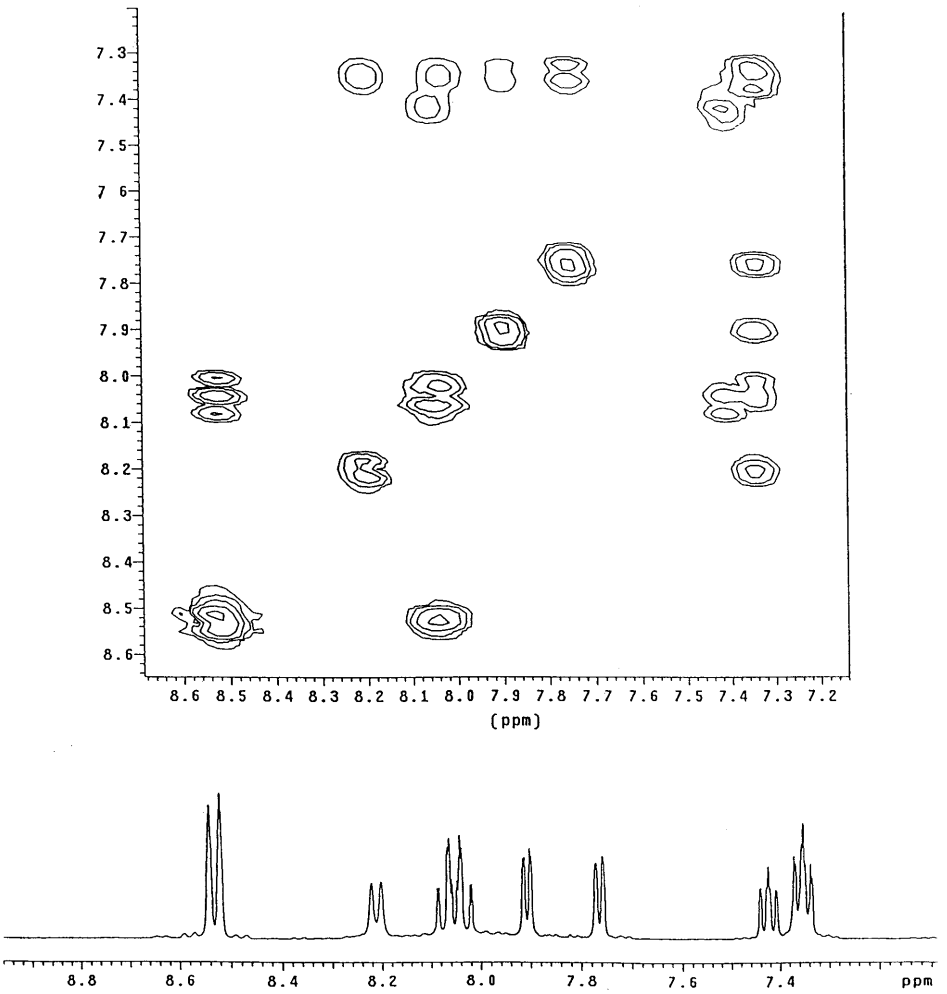

Fig. 3. ^{1}H-NMR spectrum and COSY of $[Ru(bpy)_2(dcbpy\text{-}H)^+$.

Table 6
UV–vis spectra data of complexes in CH_3CN[a]

Complexes	λ_{max} (nm), ε ($M^{-1}cm^{-1}$)		
	MLCT (dπ–π*)[b]	LC (π–π*)	LC (π–π*)
$[Ru(bpy)_2((CH_2OH)_2bpy)](PF_6)_2$	448 (1.1×10^4)	288 (5.3×10^4)	242 (2.4×10^4)
$[Ru(bpy)_2((COOCH_3)_2bpy)](PF_6)_2$	500 (4.6×10^3)	288 (5.1×10^4)	246 (1.9×10^4)
$[Ru(bpy)_2((COOC_2H_5)_2bpy)](PF_6)_2$	498 (1.0×10^4)	288 (5.6×10^4)	246 (2.2×10^4)
$[Ru(bpy)_2((COOCH_2Ph)_2bpy)](PF_6)_2$	500 (5.2×10^3)	286 (5.6×10^4)	246 (2.4×10^4)
$[Ru(bpy)_2(dcbpy\text{-}H)](PF_6)$	458 (1.2×10^4)	288 (6.4×10^4)	244 (2.2×10^4)
$[Ru(dmb)_2(dcbpy\text{-}H)](PF_6)$	458 (1.14×10^4)	288 (8.12×10^4)	244 (9.1×10^4)
$[Ru(dmb)_2(dcdmb)](PF_6)_2$	448 (1.21×10^4)	288 (6.90×10^4)	242 (7.23×10^4)
$[Ru(bpy)_3](PF_6)_2$[c]	451 (1.4×10^4)	280 (8.7×10^4)	240 (3.0×10^4)

[a] In acetonitrile; $T = 23 \pm 1$°C; λ_{max} in nm, ± 1 nm; $\varepsilon = M^{-1}\ cm^{-1}$, error = ± 0.1.
[b] Lowest energy transition. See text for details.
[c] See Ref. [59].

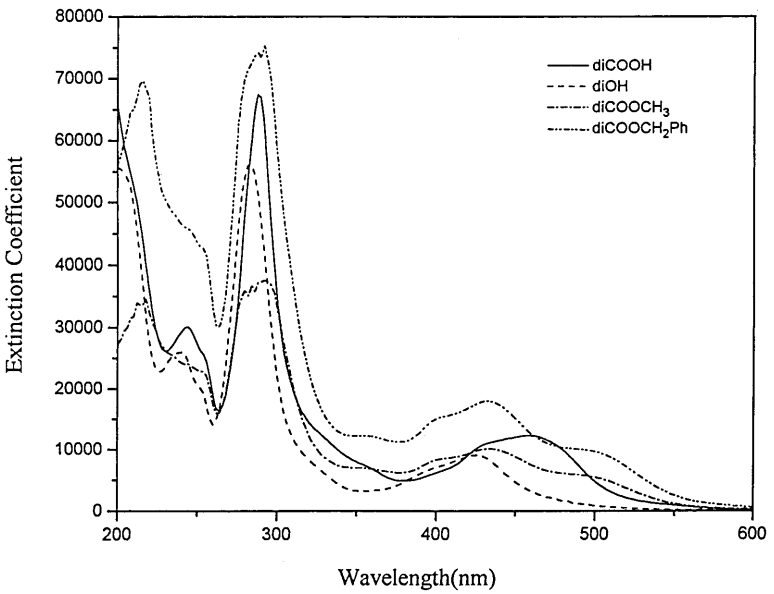

Fig. 4. UV–vis spectra of $[(bpy)_2Ru(3,3'\text{-}X,X\text{-}2,2'\text{-}bpy)]^{2+}$ in acetonitrile, X,X = 3-COO-3′-COOH, (—), CH_2OH (- - -), 3,3′-$COOCH_3$ (···), 3,3′-$COOCH_2Ph$ (··· - ···).

3.6. Electrochemistry

The oxidation and reduction potentials for all the complexes were determined by cyclic voltammetry. Redox potentials for all the complexes are tabulated in Table 7. Cyclic voltammograms of all complexes were obtained in dry acetonitrile using TBAH as the electrolyte with a scan rate of 100 mV s^{-1}. The observed couples

were all 'reversible', where the reversibility as used here implied that the separation between the anodic and the cathodic peak potentials was less than 100 mV for a one-electron process and no degradation products were observed on the following scan [38]. The $E_{1/2}$ values were determined by the equation $E_{1/2} = (E_{anodic} + E_{cathodic})/2$. The values of ΔE were calculated by subtraction of cathodic potentials from anodic potentials for a specific redox couple. The general behavior was very similar to that of analogous ruthenium complexes, and the assignment of the various couples followed directly from previous reports [39–42] and are noted by Eqs. (2)–(5).

$$[Ru(II)(bpy)(bpy)(X,X\text{-}bpy)]^{2+} - e^- \rightarrow [Ru(III)(bpy)(bpy)(X,X\text{-}bpy)]^{3+} \quad (2)$$

$$[Ru(II)(bpy)(bpy)(X,X\text{-}bpy)]^{2+} + e^- \rightarrow [Ru(II)(bpy)(bpy)(X,X\text{-}bpy^-)]^{+} \quad (3)$$

$$[Ru(II)(bpy)(bpy)(X,X\text{-}bpy^-)]^{+} + e^- \rightarrow [Ru(II)(bpy)(bpy^-)(X,X\text{-}bpy^-)] \quad (4)$$

$$[Ru(II)(bpy)(bpy^-)(X,X\text{-}bpy^-)] + e^- \rightarrow [Ru(II)(bpy^-)(bpy^-)(X,X\text{-}bpy^-)]^- \quad (5)$$

The cyclic voltammograms for some of the complexes are displayed in Fig. 5. Oxidations of the ruthenium(II) center were observed in the region between $+1.22$ and $+1.40$ V for all the complexes, whereas the reduction of the three coordinated ligands was observed in the negative potential region. Reduction of the substituted bipyridine ligand occurred first, followed by the sequencial reduction of the other two bipyridine ligands. Difficulties arose in determining the reduction potentials of the carboxylic acid derivatives due to irreversible hydrogen evolution at the electrode.

Table 7
Redox properties of complexes[a,b]

Complexes	Oxidation (V)		Reductions (V)	
	$E_{1/2}(\Delta E)$		$E_{1/2}(\Delta E)$	
$[Ru(bpy)_2((CH_2OH)_2bpy)](PF_6)_2$	1.22(82)	−1.36(82)	−1.54(96)	−1.66(55)
$[Ru(bpy)_2((COOCH_3)_2bpy)](PF_6)_2$	1.35(82)	−0.92(82)	−1.46(82)	−1.68(96)
$[Ru(bpy)_2((COOC_2H_5)_2bpy)](PF_6)_2$	1.40(62)	−0.92(74)	−1.43(56)	−1.61(68)
$[Ru(bpy)_2(4,4'\text{-}(COOC_2H_5)_2bpy)](PF_6)_2$[c]	1.38	−0.93	−1.36	−1.56
$[Ru(bpy)_2((COOCH2Ph)_2bpy)](PF_6)_2$	1.38(82)	−0.88(88)	−1.41(78)	−1.59(92)
$[Ru(bpy)_2((dcbpy\text{-}H)](PF_6)$	1.36(86)	−0.60(irr)	−1.40(88)	−1.62(104)
$[Ru(bpy)_2(4,4'\text{-}(COOH)_2bpy)](PF_6)_2$[c]	1.38(96)		−1.38(96)	−1.62(150)
$[Ru(dmb)_2((dcbpy\text{-}H)](PF_6)$	1.27(100)	−0.68(irr)	−1.43(126)	[d]
$[Ru(bpy)_2((dcdmb)](PF_6)_2$	1.26(82)	−0.68(irr)	−1.48(80)	[d]
$[Ru(bpy)_3](PF_6)_2$[c]	1.28(60)	−1.32(60)	−1.52(60)	−1.78(60)

[a] All samples measured in 0.1 M TBAH–CH_3CN; error in potential was ± 0.02 V vs. SSCE.
[b] $T = 23 \pm 1$°C; scan rate = 100 mV s^{-1}; ΔE in parenthesis.
[c] See Ref. [59].
[d] Masked.

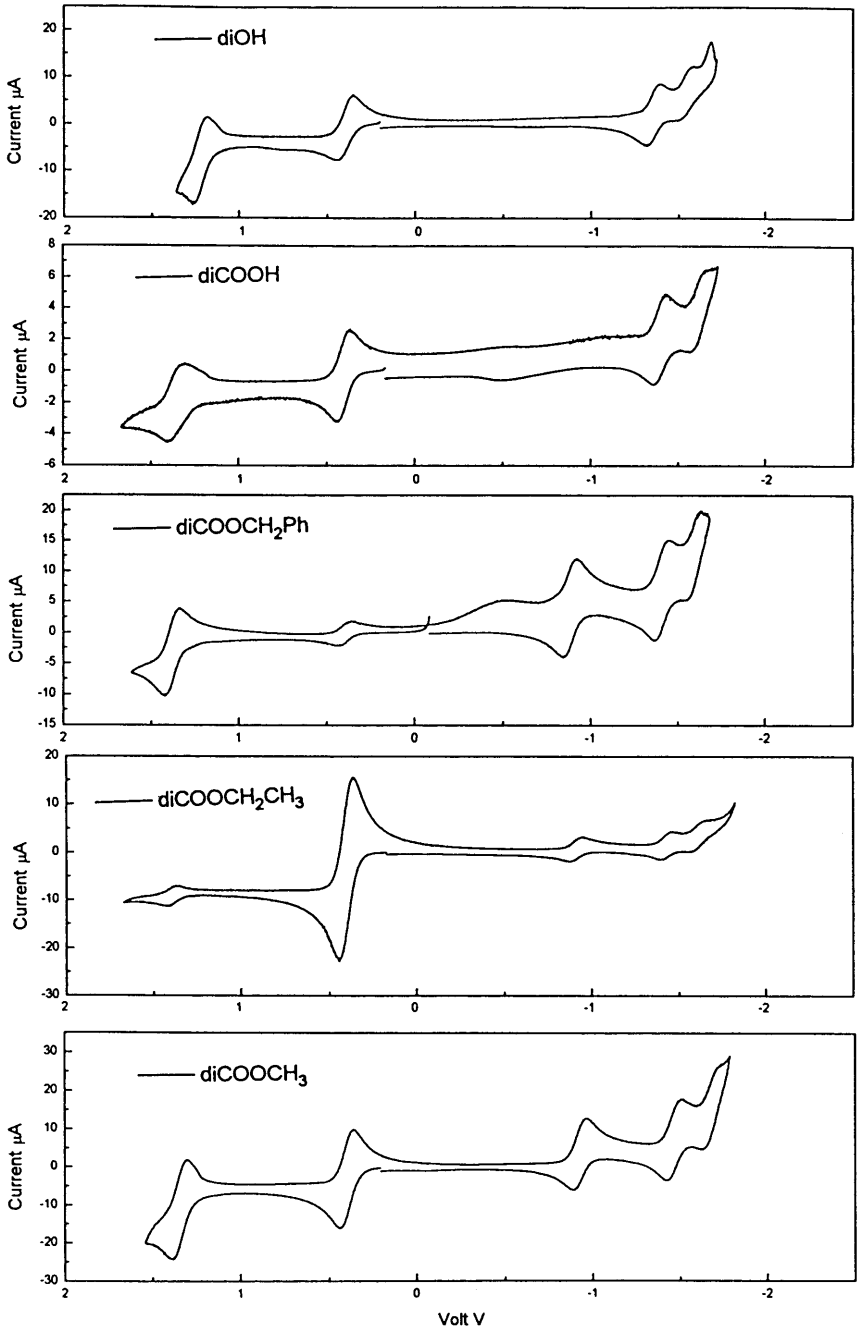

Fig. 5. Cyclic voltammograms of $[(bpy)_2Ru(3,3'\text{-}X,X\text{-}2,2'\text{-}bpy)]^{2+}$ in acetonitrile, from top to bottom: X,X = CH_2OH, 3-COO-3′-COOH, 3,3′-$COOCH_2Ph$, 3,3′-COOEt, 3,3′-$COOCH_3$.

3.7. Emission properties

Photophysical data of emission maxima, emission lifetimes, and emission quantum yields are listed in Table 8. The room temperature spectra in acetonitrile for five complexes are given in Fig. 6. All the spectra show structureless, broad peaks. Emission maxima occurred at 614, 637, 660, 711, 711 and 711 nm for $[Ru(bpy)_2((CH_2OH)_2bpy)]^{2+}$, $[Ru(bpy)_2(dcbpy\text{-}H)]^{+}$, $[Ru(dmb)_2(dcbpy\text{-}H)]^{+}$, $[Ru(bpy)_2((COOCH_3)_2bpy)]^{2+}$, $[Ru(bpy)_2((COOC_2H_5)_2bpy)]^{2+}$, and $[Ru(bpy)_2((COOCH_2Ph)_2bpy)]^{2+}$, respectively. Emission maximum follow the energy trend $[Ru(bpy)_2((CH_2OH)_2bpy)]^{2+} > [Ru(bpy)_2(dcbpy\text{-}H)]^{+} > [Ru(dmb)_2(dcbpy\text{-}H)]^{+} > [Ru(bpy)_2((COOCH_3)_2bpy)]^{2+} \sim [Ru(bpy)_2((COOC_2H_5)_2bpy)]^{2+} \sim [Ru(bpy)_2((COOCH_2Ph)_2bpy)]^{2+}$.

Emission spectra at 77 K in 4:1 EtOH–MeOH are shown in Fig. 7. The spectra differ from spectra obtained at room temperature. Firstly, the spectra showed

Table 8
Photophysical data for the ruthenium complexes

Complexes	λ_{em} (nm)[a] r.t.	λ_{em}[b] (nm) 77 K	λ_{abs} (nm)[a]	τ (ns)[a] r.t.	τ[b] (μs) 77 K	ϕ_{em}[a]
$[Ru(bpy)_2((CH_2OH)_2bpy)](PF6)_2$	614	580	448	940	4.92	2.3×10^{-3}
$[Ru(bpy)_2((COOCH_3)_2bpy)](PF_6)_2$	711	650	500	258	1.88	1.2×10^{-3}
$[Ru(bpy)_2(4,4'\text{-}(COOCH_3)_2bpy)](PF_6)_2$[c]	660		475	615		4.5×10^{-2}
$[Ru(bpy)_2((COOC_2H_5)_2bpy)](PF_6)_2$	711	650	498	271	1.90	1.1×10^{-3}
$[Ru(bpy)_2((COOCH_2Ph)_2bpy)](PF_6)_2$	711	651	500	425	1.91	4.4×10^{-4}
$[Ru(bpy)_2(dcbpy\text{-}H)](PF_6)$	637	597	458	534	4.10	2.2×10^{-3}
$[Ru(dmb)_2(dcbpy\text{-}H)](PF_6)$	660	617	458	671	4.23	2.6×10^{-3}
$[Ru(dmb)_2(dcdmb)](PF_6)_2$		625	458			4.6×10^{-2}
$[Ru(bpy)_2(3,5\text{-}(COOH)_2bpy)](PF_6)_2$[d]		637	460	846	2.86	
$[Ru(bpy)_2(4,4'\text{-}(COOH)_2bpy)](PF_6)_2$[e]	655		460	1060[d]		3.9×10^{-2}[f]
$[Ru(bpy)_3](PF_6)_2$[g]	600	582	451	890	5.20	6.2×10^{-2}

[a] In acetonitrile solution: $T = 298$ K; error $= \pm 2$ nm; $\lambda_{ex} = 450$ nm.
[b] Lifetimes were measured in 4:1 C_2H_5OH–CH_3OH (v/v) at 77 K.
[c] See Ref. [60].
[d] See Ref. [61].
[e] See Ref. [62].
[f] In H_2O: see Ref. [63].
[g] See Ref. [59].

structure, a peak and a shoulder. Secondly, the emission maxima were shifted to higher energy and occurred at 580, 597, 617, 625, 651, 651 and 651 nm for $[Ru(bpy)_2((CH_2OH)_2bpy)]^{2+}$, $[Ru(bpy)_2(dcbpy\text{-}H)]^{+}$, $[Ru(dmb)_2(dcbpy\text{-}H)]^{+}$, $[Ru(dmb)_2(dcdmb)]^{2+}$, $[Ru(bpy)_2((COOCH_3)_2bpy)]^{2+}$, $[Ru(bpy)_2((COOC_2H_5)_2\text{-}bpy)]^{2+}$, $[Ru(bpy)_2((COOCH_2Ph)_2\text{-}bpy)]^{2+}$, respectively. The blue shift was between 30 and 60 nm compared to the emission maxima at room temperature. The values showed a trend consistent with those found in other measurements with the energy order being $[Ru(bpy)_2((CH_2OH)_2bpy)]^{2+} > [Ru(bpy)_2(dcbpy\text{-}H)]^{+}, > [Ru(dmb)_2(dcbpy\text{-}H)]^{+} > [Ru(dmb)_2(dcdmb)]^{2+} > [Ru(bpy)_2((COOCH_3)_2bpy)]^{2+} \sim [Ru(bpy)_2((COOC_2H_5)_2\text{-}bpy)]^{2+} \sim [Ru(bpy)_2((COOCH_2Ph)_2\text{-}bpy)]^{2+}$.

The room temperature emission lifetimes for the complexes were measured in acetonitrile and were 940, 671, 534 and 258 ns for $[Ru(bpy)_2((CH_2OH)_2bpy)]^{2+}$, $[Ru(dmb)_2(dcbpy\text{-}H)]^{+}$, $[Ru(bpy)_2(dcbpy\text{-}H)]^{+}$, $[Ru(bpy)_2((COOCH_3)_2bpy)]^{2+}$, respectively. The emission lifetimes at 77 K were measured in 4:1 EtOH–MeOH and the lifetimes were 4.92, 4.23, 4.10 and 1.9 μs for $[Ru(bpy)_2((CH_2OH)_2bpy)]^{2+}$, $[Ru(dmb)_2(dcbpy\text{-}H)]^{+}$, $[Ru(bpy)_2(dcbpy\text{-}H)]^{+}$ and $[Ru(bpy)_2((ester)_2bpy)]^{2+}$, respectively. Emission lifetimes followed the same trend as emission energies with $[Ru(bpy)_2((CH_2OH)_2bpy)]^{2+} > [Ru(dmb)_2(dcbpy\text{-}H)]^{+} \sim [Ru(bpy)_2(dcbpy\text{-}H)]^{+} > [Ru(bpy)_2((COOCH_3)_2bpy)]^{2+} \sim [Ru(bpy)_2((COOC_2H_5)_2bpy)]^{2+} \sim [Ru(bpy)_2((COOCH_2Ph)_2bpy)]^{2+}$ both at room temperature and at 77 K.

The emission quantum yields at room temperature were measured in acetonitrile and the data are listed in Table 8. The emission quantum yields were calculated by

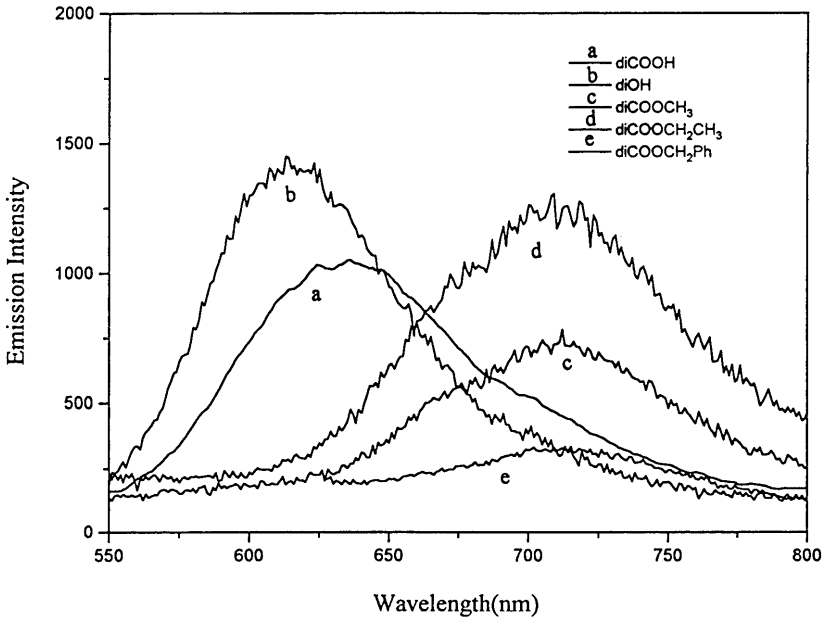

Fig. 6. Emission spectra of $[(bpy)_2Ru(3,3'\text{-}X,X\text{-}2,2'\text{-}bpy)]^{2+}$ in acetonitrile at r.t., X,X = (a) 3-COO-3′-COOH, (b) CH_2OH (c) 3,3′-$COOCH_3$ (d), 3,3′-COOEt, (e) 3,3′-$COOCH_2Ph$.

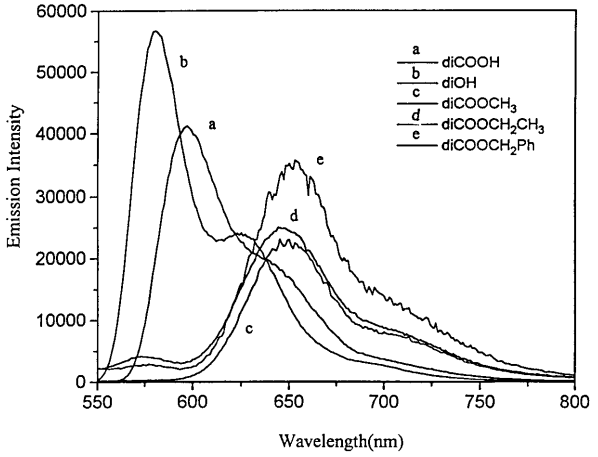

Fig. 7. Emission spectra of $[(bpy)_2Ru(3,3'\text{-}X,X\text{-}2,2'\text{-}bpy)]^{2+}$ in 4:1 $C_2H_5OH-CH_3OH$ at 77 K, X,X = (a) 3-COO-3′-COOH, (b) CH_2OH, (c) 3,3′-$COOCH_3$, (d) 3,3′-COOEt, (e) 3,3′-$COOCH_2Ph$.

comparison with the well documented emission quantum yield for $[Ru(bpy)_3]^{2+}$ [25]. Emission quantum yields fall in the $(1-3) \times 10^{-3}$ range for complexes with the exception of $[Ru(bpy)_2((COOCH_2Ph)_2bpy)]^{2+}$, which is an order of magnitude smaller.

4. Discussion

4.1. Preparations

The preparation of the ligands utilized procedures, which smoothly resulted in the formation of the desired products. Highest yields of 3,3′-$(COOH)_2$bpy required the slow addition of $KMnO_4$ at room temperature to an alkaline solution followed by refluxing the solution to oxidize 1,10-phenanthroline to the desire product. Addition of $KMnO_4$ to a refluxing alkaline solution resulted in a decreased yield of 3,3′-$(COOH)_2$bpy and an increased yield of 4,5-diazafluorenone, one of the byproducts formed in the reaction where $KMnO_4$ was added at room temperature. Ring opening of 4,7-dimethyl-1,10-phenanthroline was favored under mild conditions; the ring opens first rather than oxidation of the 4,7-dimethyl substituents. The ester derivatives were formed by addition of two catalysts to the appropriate alcohol solution containing 3,3′-$(COOH)_2$bpy. One catalyst deprotonated the acid groups (e.g. *N*-methylmorpholine); the other catalyst underwent addition to the deprotonated carboxyl group (e.g. methylchloroformate) to yield a good leaving group which was then replaced by the solvent resulting in formation of the derivatized ester ligand. Formation of 3,3′-$(CH_2OH)_2$bpy was produced directly from the ester derivative rather than by reduction of 3,3′-$(COOH)_2$bpy. The reagent found accept-

able for affecting this transformation was sodium bis(2-methoxyethoxy) aluminum hydride.

The preparation of the complexes followed typical published procedures where the ligand was reacted with $Ru(bpy)_2Cl_2$ or $Ru(dmb)_2Cl_2$ to yield the mixed ligand complexes. Since the complexes contained two ionizable protons as noted by Eq. (6), various forms of the complexes were potentially isolable.

$$Ru(COOH)_2 \overset{K_1}{\rightleftharpoons} Ru(COOH)(COO^-) \overset{K_2}{\rightleftharpoons} Ru(COO^-)_2 \quad (6)$$

In the case of the 4,4′- or 3,5-dicarboxyl derivatives, $[Ru(bpy)_2(4,4'\text{-}(COOH)_2\text{-}bpy)]^{2+}$ [43–49] and $[Ru(bpy)_2(3,5\text{-}(COOH)_2bpy)]^{2+}$ [44,45] were isolated. However, here the singly deprotonated $[Ru(bpy)_2(dcbpy\text{-}H)]^+$ and $[Ru(dmb)_2(dcbpy\text{-}H)]^+$ species were obtained, although in the case of $[Ru(dmb)_2(dcdmb)]^{2+}$, the doubly protonated form was isolated by precipitation with HPF_6. The conditions under which the complexes were isolated appears to be the key factor since the pK_a values for the first deprotonation step are 0.7 for the 3,5-dicarboxyl derivative [50,51], 1.85 for the 4,4′-dicarboxyl complex [41] and ~ 2 for the 3,3′-derivatives isolated here [52].

4.2. X-ray structure

The X-ray structure of the ruthenium(II) coordination sphere revealed bond lengths similar to those of other ruthenium bipyridine complexes [53,54]. It was particularly surprising to find similar Ru–N bond distances for coordinated $3,3'\text{-}(COOCH_3)_2bpy$ (2.055 (6) and 2.059(6) Å) as for those found for $[Ru(bpy)_3]^{2+}$ (2.056 Å). The bite angles of the coordinated ligands (N–Ru–N) were also similar to those found in $[Ru(bpy)_3]^{2+}$ (78°) [53]. The dihedral angles for the two unsubstituted bipyridine ligands fell in the range (2–6°) normally found for such structures. The only unusual structural property was the large dihedral angle of 28.1° found for the 3,3′-substituted ligand.

4.3. Physical and photophysical properties of the ruthenium complexes

The physical and photophysical properties of the complexes reported here can be compared to complexes containing like substituents in other ring positions and can be assessed by the Hammett σ function approach [55]. Complexes with substituents in the 3,3′ positions also contain an added steric problem due to a twist of $\sim 30°$ about the carbon–carbon bridge head. The following addresses these concerns.

First, within the 3,3′ series, according to the electron donor–electron withdrawal concept, the CH_2OH group is an electron donor whereas the COOH and COOR groups are electron acceptors. Deprotonated carboxyl groups, on the other hand, have Hammett constants comparable to hydrogen, which is taken to be the standard [56]. Consequently, relative to $[Ru(bpy)_3]^{2+}$, the electron donor group shifts the redox potentials for $[Ru(bpy)_2((CH_2OH)bpy)]^{2+}$ to more negative values and the MLCT absorption to higher energy. The ester groups result in the opposite effect, red-shifting the absorptions of the ruthenium complexes to 485 nm and the

redox potentials to more positive values. Since at least one of the acid groups was deprotonated, the MLCT absorption for the carboxyl complexes were similar in energy to that of $[Ru(bpy)_3]^{2+}$. Similar effects were found for emission properties where emission decay lifetimes of the 3,3′-substituted bipyridine complexes followed the energy gap law [57,58]. A plot of emission lifetimes versus E_{em} was linear with a correlation coefficient of 0.97. The plot was basically composed of three points since the ester derivatives gave almost the same results.

The second of these concerns, steric problems, can be made by comparison of properties for 3,3′ derivatives to analogous 4,4′-$(COOR)_2$bpy (R = COOH and $COOCH_3$) [37–43] and 3,5-$(COOH)_2$bpy [50,51] ruthenium complexes. Comparison of the photophysical properties of $[Ru(bpy)_2((COOCH_3)_2bpy)]^{2+}$ to those of $[Ru(bpy)_2(4,4'\text{-}(COOCH_3)_2bpy)]^{2+}$ clearly indicates a red shift in the absorption from 475 to 500 nm, a red shift in room temperature emission energy from 660 to 711 nm, and a decrease in emission lifetime from 615 to 258 ns. The three acid complexes, $[Ru(bpy)_2(3,3'\text{-}(COOH)_2bpy)]^{2+}$, $[Ru(bpy)_2(3,5\text{-}(COOH)_2bpy)]^{2+}$ and $[Ru(bpy)_2(4,4'\text{-}(COOH)_2bpy)]^{2+}$ absorb near 450 nm, emit in the energy sequence $[Ru(bpy)_2(3,5\text{-}(COOH)_2bpy)]^{2+}$ (637 nm) > $[Ru(bpy)_2(4,4'\text{-}(COOH)_2bpy)]^{2+}$ (655 nm) > $[Ru(bpy)_2(3,3'\text{-}(COOH)_2bpy)]^{2+}$ (660nm) with emission lifetimes of 846, 1060 and 671 ns, respectively. The major change, however, is in the emission quantum yields, which are about an order of magnitude less for the 3,3′-substituted derivatives. The $\sim 30°$ twist about the carbon–carbon bridge-head does have a rather dramatic effect by disrupting the π conjugation of the bipyridine ligand diminishing the photophysical properties of the electron donor–acceptor systems.

5. Supplementary material

Crystallographic data (30 pages) including experimental details, atomic coordinates, B_{iso}/B_{eq}, anisotropic displacement parameters, bond lengths, bond angles, torsion angles, non-bonded contacts out to 3.6 Å and least-square planes are available from the author.

Acknowledgements

We thank the Office of Basic Energy Sciences of the United States Department of Energy for support of this investigation and the National Science Foundation for the 400 MHz NMR and the laser equipment.

References

[1] A. Juris, V. Balzani, F. Barigelletti, S. Campagna, P. Belser, A. von Zelewsky, Coord. Chem. Rev. 84 (1988) 85.
[2] V. Balzani, A. Juris, M. Venturi, S. Campagna, S. Serroni, Coord. Chem. Rev. 96 (1996) 759.

[3] K. Kalyanasundaram, Photochemistry of Polypyridine and Porphyrin Complexes, Academic Press, London, 1992.
[4] A. Hegfelt, M. Grätzel, Chem. Rev. 95 (1995) 49.
[5] T.J. Meyer, Acc. Chem. Res. 22 (1989) 163.
[6] V. Balzani, S. Campagna, G. Denti, A. Juris, S. Serroni, M. Venturi, Acc. Chem. Res. 31 (1998) 26.
[7] V. Grosshenny, A. Harriman, R. Ziessel, Angew. Chem. Int. Ed. Engl. 34 (1995) 1100.
[8] J.R. Shaw, G.S. Sadler, W.F. Wacholtz, C.K. Ryu, R.H. Schmehl, New. J. Chem. 20 (1996) 749.
[9] C.A. Bignozzi, J.R. Schoonover, F. Scandola, Prog. Inorg. Chem. 44 (1997) 1.
[10] S.M. Molnar, G. Nallas, J.S. Bridgewater, K.J. Brewer, J. Am. Chem. Soc. 116 (1994) 5206.
[11] D.P. Rillema, R.W. Callahan, K.B. Mack, Inorg. Chem. 21 (1982) 2589.
[12] D.P. Rillema, K.B. Mack, Inorg. Chem. 21 (1982) 3451.
[13] R. Sahai, D.P. Rillema, J. Chem. Soc. Chem. Commun. (1986) 1133.
[14] R. Sahai, L. Morgan, D. Paul Rillema, Inorg. Chem. 27 (1988) 3495.
[15] D.P. Rillema, W.J. Dressick, T.J. Meyer, J. Chem. Soc. Chem. Commun. (1980) 247.
[16] W.J. Dressick, T.J. Meyer, D. Durham, D.P. Rillema, Inorg. Chem. 21 (1982) 3451.
[17] Y. Wang, D.P. Rillema, Tetrahedron Lett. 38 (1997) 6627.
[18] Y. Wang, D.P. Rillema, Inorg. Chem. Commun. 1 (1998) 27.
[19] Y. Wang, G.Y. Zheng, W.J. Perez, C.L. Huber, D.P. Rillema, Inorg. Chem. 37 (1998) 2227.
[20] Y. Wang, W.J. Perez, D.P. Rillema, Inorg. Chem. 37 (1998) 2051.
[21] B.P. Sullivan, D.J. Salmon, T.J. Meyer, Inorg. Chem. 17 (1978) 3334.
[22] G.F. Smith, F.T. Richter, Phenanthroline and Substituted Phenanthroline, G.F. Smith Chemical, Columbus, OH, 1944, p. 20.
[23] D. Aziz, J.G. Breckenridge, Can. J. Res. Sect. B 28 (1950) 26.
[24] J. Rebek, J.E. Trend, R.V. Wattley, S. Chakravorti, J. Am. Chem. Soc. 101 (1979) 4333.
[25] J.M. Calvet, J.V. Caspar, R.A. Binstead, T.D. Westmoreland, T.J. Meyer, J. Am. Chem. Soc. 104 (1982) 6620.
[26] J.N. Demas, G.A. Crosby, J. Phys. Chem. 75 (1971) 991.
[27] SIR92: A. Altomare, M. Cascarano, C. Giacovazzo, A. Guagliardi, J. Appl. Cryst. 26 (1999) 343.
[28] TEXSAN: Crystal Structure analysis Package, Molecular Structure Corporation, 1985 and 1992.
[29] DIFABS: N. Walker, Stuart, Acta Crystallogr. Sect. A 39 (1983) 158.
[30] Scatterring factors: D.T. Cromer, J.T., Waber, International Tables for X-ray Crystallography, vol. IV, Kynoch, Birmingham, UK, 1974, Table 2.2A.
[31] Anomalous dispersion factors: D.C. Creagh, W.J. McAuley, in: A.J.C. Wilson (ed.), International Tables for X-ray Crystallography, vol. C, Kluwer, Boston, 1992, Table 4.2.6.8, pp. 219–222.
[32] C.K. Johnson, ORTEP — A FORTRAN Thermal Ellipsoid Plot Program. Technical Report ORNL-5138, Oak Ridge, TN, 1976.
[33] K. Kalyanasundaram, Coord. Chem. Rev. 46 (1982) 159.
[34] E.A. Seddon, K.R. Seddon, The Chemistry of Ruthenium, Elsevier, Amsterdam, 1984.
[35] F. Felix, J. Ferguson, J.A. Gudel, A. Ludi, J. Am. Chem. Soc. 102 (1980) 4096.
[36] E.M. Kober, T.J. Meyer, Inorg. Chem. 21 (1982) 3967.
[37] Abbreviations are used, for example, Ru($(CH_2OH)_2$bpy) for $[(bpy)_2Ru(3,3'\text{-}(CH_2OH)_2bpy)]^{2+}$.
[38] A.K.R. Unni, L. Elias, H.I. Schift, J. Phys. Chem. 67 (1963) 1216.
[39] E.M. Kober, J.V. Caspar, B.P. Sullivan, T.J. Meyer, Inorg. Chem. 27 (1988) 4587.
[40] D.A. Buckingham, F.P. Dwyer, A.M. Sargeson, Inorg. Chem. 5 (1966) 1243.
[41] T. Matsumura-Inoye, T.J. Tominaga-Morimoto, Electroanal. Chem. Interfacial Electrochem. 93 (1978) 127.
[42] S. Roffia, M.J. Ciano, Electroanal. Chem. Interfacial Electrochem. 100 (1979) 809.
[43] P.J. Giordano, C.R. Bock, M.S. Wrighton, L.V. Interante, R.F.X. Williams, J. Am. Chem. Soc. 99 (1977) 3187.

[44] W.R. Cherry, J.L. Henderson, Jr., Inorg. Chem. 23 (1984) 983.
[45] P.A. Lay, W.H.F. Sasse, Inorg. Chem. 23 (1984) 4123.
[46] T. Shimidzu, T. Iyoda, K. Izaki, J. Phys. Chem. 89 (1985) 642.
[47] Md.K. Nazeeruddin, K. Kalyanasundaram, Inorg. Chem. 28 (1989) 4251.
[48] J.G. Vos, Polyhedron 11 (1992) 2285.
[49] K. Kalyanasumdaram, Md.K. Nazeeruddin, M. Gratzel, G. Viscardi, P. Savarino, E. Barni, Inorg. Chim. Acta 198 (1992) 831.
[50] S.R.L. Fernando, M.Y. Ogawa, J. Chem. Soc. Chem. Commun. (1996) 637.
[51] S.R.L. Fernando, U.S.M. Maharoof, K.D. Deshayes, T.H. Kinstle, M.Y. Ogawa, J. Am. Chem. Soc. 118 (1996) 5783.
[52] B.-Z. Shan, D.P. Rillema, unpublished data.
[53] D.P. Rillema, D.S. Jones, H.A. Levy, J. Chem. Soc. Chem. Commun. (1979) 849.
[54] D.P. Rillema, D.S. Jones, C. Woods, H. Levy, Inorg. Chem. 31 (1992) 2935.
[55] E.S. Gould, Mechanism and Structure in Organic Chemistry, Holt, Rinehart and Winston, New York, 1959, p. 221.
[56] A.J. Gordon, R.A. Ford, The Chemists Companion, Wiley, New York, 1972, pp. 145–147.
[57] R. Englman, J. Jortner, Mol. Phys. 18 (1970) 145.
[58] R.F. Freed, J. Jortner, J. Chem. Phys. 52 (1970) 6272.
[59] A. Juris, V. Balzani, F. Barigelletti, S. Campagna, P. Belser, A. von Zelewsky, Coord. Chem. Rev. 84 (1988) 85.
[60] A. Harriman, J. Chem. Soc. Chem. Commun. (1977) 777.
[61] S.R.L. Fernando, W.S.M. Maharoof, K.D. Deshayes, T.H. Kinstle, M.Y. Ogawa, J. Am. Chem. Soc. 118 (1996) 5783.
[62] P.J. Giordano, C.R. Bock, M.S. Wrighton, L.V. Interrane, R.F.X. Williams, J. Am. Chem. Soc. 99 (1977) 3187.
[63] W.R. Cherry, L.J. Henderson, Jr., Inorg. Chem. 23 (1984) 983.